Manufacturing Rev. **9**, 10 (2022)

https://doi.org/10.1051/mfreview/2022008

Manufacturing Review
Available online at:
https://mfr.edp-open.org

RESEARCH ARTICLE OPEN ACCESS

Optimization and prediction of hardness, wear and surface roughness on age hardened stellite 6 alloys

Karthik S.R.[1], Neelakanta V. Londe[1], Raviraj Shetty[2,*], Rajesh Nayak[2], and Adithya Hedge[2]

[1] Department of Mechanical Engineering, Mangalore Institute of Technology and Engineering, Moodabidri, Karnataka, India
[2] Department of Mechanical and Manufacturing Engineering, Manipal Institute of Technology, Manipal Academy of Higher Education, Manipal 571604, Karnataka, India

Received: 28 October 2021 / Accepted: 23 February 2022

Abstract. Growing demand for Stellite 6 alloys due to its attractive properties such as superior strength, toughness, wear resistance, fracture resistant characteristics, and their exceptional resistance to corrosion has made them applicable in industrial as well as commercial applications, such as aerospace industries, nuclear waste storage, automobile industries and surgical implantation. However, in spite of these applications, automotive part manufacturers mainly (Bearing Materials) are looking for a comprehensive study, such as mechanics of friction and the relationship between friction and wear. Hence in this paper, an attempt has been made to study the tribological behavior such as wear characterization and surface roughness of age hardened Stellite 6 alloys. The main objective of the research is to determine the favorable tribological conditions for improving wear resistant properties and surface roughness on age hardened Stellite 6 alloys. Hence two body wear study and surface roughness study during Wire Electric Discharge Machining (WEDM) of age hardened Stellite 6 alloys based on Analysis of Variance (ANOVA), Taguchi's Design of Experiment (TDOE), Response Surface Methodology(RSM) and Desirability Functional Analysis (DFA) have been used to achieve this goal. From the study it is observed that optimum values for improving hardness, wear and surface roughness values can be easily achieved with less time and cost by adopting the said techniques. •From microstructural observation, as the peak current increases there is larger amount of dendritic carbides and cracking of carbides due to high plastic deformation resulting in thermal softening of Stellite 6 alloy during wire electric discharge machining resulting in better surface roughness values. The second-order model for hardness, wear and surface roughness using response surface methodology can be adopted for predicting for hardness, wear and surface roughness in any experimental domain.

Keywords: Stellite 6 alloys / hardness / wear / surface roughness / WEDM / ANOVA / TDOE / RSM / DFA

1 Introduction

Over last 12 decades, Stellite alloys have come into existence and have been developed by Elwood P. Haynes, for producing various component parts of steam engines and internal combustion engines and named these alloys as "Stellites" [1]. The most important characteristics of these alloys are its hardness, high wear resistance, corrosion resistance and high temperature withstanding capacity compared to other metals and alloys. "Stellite alloys are a class of cobalt-chromium "super-alloys" made up of complex carbides in an alloy matrix that are primarily created for excellent wear resistance as well as enhanced chemical and corrosion resistance in severe environments". Because of its extremely high melting points, cobalt and chromium are suited for a wide range of applications, from "extreme cutting tools to hot section alloy coatings in gas turbines". To provide even better performance for specific applications, they may also contain molybdenum or tungsten, as well as a small amount of carbon. Metallographic microstructure of Stellite 6 alloy is given in Figure 1.

Because of its superior mechanical, tribological, adhesive, and abrasive wear resistance qualities, stellite alloys have been employed in a wide range of industrial applications. "The Stellite alloys are attractive in a number of applications due to the crystallographic nature of cobalt, the solid-solution-strengthening effects of chromium, tungsten, and molybdenum, the creation of metal carbides, and the corrosion resistance due to the presence of chromium". High-carbon alloys and medium-carbon alloys

* e-mail: rr.shetty@manipal.edu

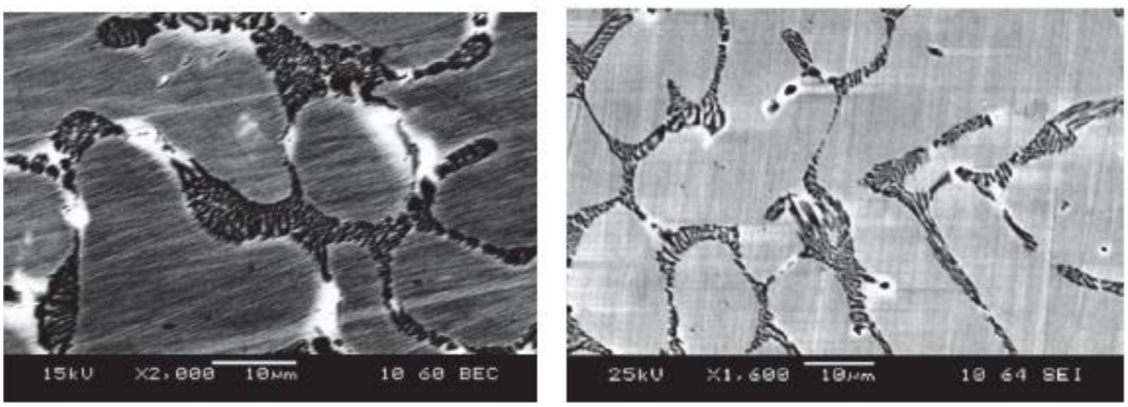

Fig. 1. "Metallographic microstructure of the Stellite 6 alloy" [2].

are the two types of stellite alloys [3]. Depending on the application, stellite alloys are made via casting, powder metallurgy, laser cladding, hot forging, and hard-faced deposit. Because stellite alloy is a tough to machine material, it is always possible to use non-traditional machining techniques such as EDM, WEDM, and ultrasonic machining instead of conventional machining [4–7]. Further Stellites are often added to stainless steel or mild steel substrates as a coating, powder, or casting. Stellite alloy has found use in rolling element bearings, inline jet engine valves, landing gear, and actuation equipment due to the combination of complex carbides in an alloy matrix. [8–11]. Stellite alloy is considered to be hard to machine material due to its high hardness and toughness compared to other metal and alloys. Hence the machining cost of these materials has become more expensive. Further, "Stellite alloys consisting of hard carbides, non-homogeneous distribution of carbides, non-homogeneous crystal structure, high heat affected zone, more residual stress induced, low thermal conductivity results in poor machinability" [12–14]. Hence researchers are concentrating on identifying optimal machining parameters achieve the better surface roughness with minimum wear during machining of Stellite alloys. It was also observed that due to increased hardness and toughness of Stellite alloy, results in "heat generation in the cutting zone resulting in metallographic phase transformation". [15] in their research they had experimented with "usage of Stellite alloys, such as Stellite 31, Stellite 6, Stellite 6B, Stellite 3 and Stellite 19" in order to "increase the life of certain aircraft engine components such as flare castings, spacer sleeves, rod end bearings, ball bearings, bearing races, fuel nozzles, swirlers, washers, engine vanes, bearing supports and other static structural parts followed by Stellite 21 and Stellite 31 alloys for producing cast turbine blades which are used in military piston engines on a number of aircraft". They also concluded that non-homogeneous distribution of hard carbide, lower heat conductivity, and high hardness contributed to poor machinability properties of Stellite 6 alloy. In their research [16], they had processed Stellite 6 by wire arc additive manufacturing process. Further, "the effect of stress relief annealing on the mechanical performance the fabricated Stellite 6 part was studied and compared with the corresponding casting part". They concluded that Stellite 6 manufactured through additive manufacturing process exhibited 7–8 HRC more hardness and 150MPa higher tensile and ultimate strength than the cast part. While working on Stellite 6 alloys discovered that the formation of hard carbides in Stellite alloys provided sliding wear and abrasion wear resistance [17]. They also suggested that Stellite alloys were found to exhibit excellent metal-on-metal anti-galling behavior. In their work [18], they had investigated about the "influences of EDM machining conditions on micro-EDM characteristics". Their experimental results showed that the "voltage and current of the pulse exert strongly to the machining properties". They concluded that "shorter EDM pulses were more efficient to make a precision part with a higher MRR". In their study of Stellite 6 [19], they discovered that residual stresses on the machined surface had a significant impact on the alloy's fatigue life, crack resistance, stress corrosion resistance, static strength, and magnetic characteristics. According to their research on Stellite alloys [20], residual tensile stresses lower the fatigue strength of machined parts, shortening the actual product life. Residual stresses develop within a depth of 50 μm of the surface when sharp tools are used, and up to 500 μm when worn tools are used. While working with the Stellite 6 alloy [21], they discovered that residual stresses are more common when using uncoated tools rather than coated tools. Reference [22] had analyzed "residual stresses on turbine disks (made of Stellite 6) of jet engines that were machined under various cutting conditions. They concluded that the worst condition was at the 0.06 mm depth of cut because this produced the lowest value of compressive residual stress (–100 MPa) and the highest value of tensile residual stress (800 MPa)" [23]. They investigated the effect of adding silicon to Stellite 6 on its hardness and wear resistance at high temperatures in their research. They found that adding silicon increased the hardness of Stellite 6 and increased the wear resistance of Stellite 6 at low temperatures (below 100 °C), but decreased it at high temperatures. Furthermore, it was discovered that as the temperature rose, the material's wear resistance reduced [24]. In his work on electric discharge machining of Stellite alloys, he discovered that "die-sinking EDM presented an extremely low MRR in the finishing process. Further, he found that the MRR at good

Table 1. Chemical composition of Stellite 6 alloy.

Element	Composition
Co	57%
Cr	32%
W	13%
C	3%
Si	1.20%
Fe	1%
Ni	1%

surface roughness levels (1.1–3.8 μm Ra) could be improved through milling EDM due to its inherent good flushing conditions (small contact area, high flushing pressure through the electrode and rotation of the electrode)" [25]. They examined the machining characteristics of Stellite 6 using kerosene and distilled water as dielectrics in their investigation. They discovered that when machining in distilled water rather than kerosene, the MRR is higher and the relative electrode wear ratio is lower. Furthermore, when distilled water was used as the dielectric, a greater amount of particles and micro fractures were discovered. References [26–32] carried out research on machining of metals, composites and alloys using TDOE and RSM as statistical tools. The suggested that these statistical tools can be effectively used for optimization and prediction of machining output parameters. Hence in this paper hardness, wear and surface roughness study of age hardened Stellite 6 alloys based on "Taguchi's Design of Experiment, Response Surface Methodology and Desirability Functional Analysis" has been discussed.

2 Methodology

Stellite 6 alloy having hardness value of 395 H_v is the work piece material and its chemical composition are given in Table 1. The Stellite 6 workpiece was supplied by Baoji Yongshegtai Industry Co., Ltd China and procured through HAL, Bangalore. The workpiece material and microstructure of the Stellite 6 alloy is shown in Figures 2 and 3.

The Stellite 6 alloy in the for cylindrical bar of diameter 10 mm x 20 mm samples are heat treated at 950 °C for 3 h followed by water quenching at room temperature. Finally, the specimens are aged at 200 °C to 400 °C by varying the time 2–6 h and the hardness is checked using "Matsuzawa Vickers hardness (Model: MMT-X7A, Matsuzawa Co., Ltd. Japan) testing machine with an indentation load of 50 kg allowing dwell time of 15 s for indentation. At least five indentations were taken for each specimen, and the average value was reported for of Vickers hardness was reported for Stellite 6 alloy specimens". The experiments are based on Taguchi's L_{16} orthogonal array (larger the better characteristic for hardness). The levels and factors selected for age hardening based on design of experiments is shown in Table 2.

Two body wear tests were carried out by pin on disc wear testing machine. The pin material was Stellite 6 alloy. The disc material was EN-31 steel with a hardness of 640 H_v. The pin specimens were square of 10 mm and a height of 30 mm. The disc specimens were cylinders with an outer diameter of 100 mm and a thickness of 8 mm. The difference in the mass measured before and after the test gives the wear of the specimen. The mass loss of the pin (specimen) was measured in an electronic weighing machine with a least count of 0.001 g. The ratio of mass losses was defined as wear rate. Stellite 6 alloy under different Load (N), Sliding Speed (m/s) based on L_9 orthogonal array based Taguchi's design of experiments as shown in Table 3 has been conducted followed by Mathemetical model using RSM" (Tab. 4).

The wire electric discharge machining experiments of Stellite 6 alloy cylindrical specimen size of 20 mm thickness

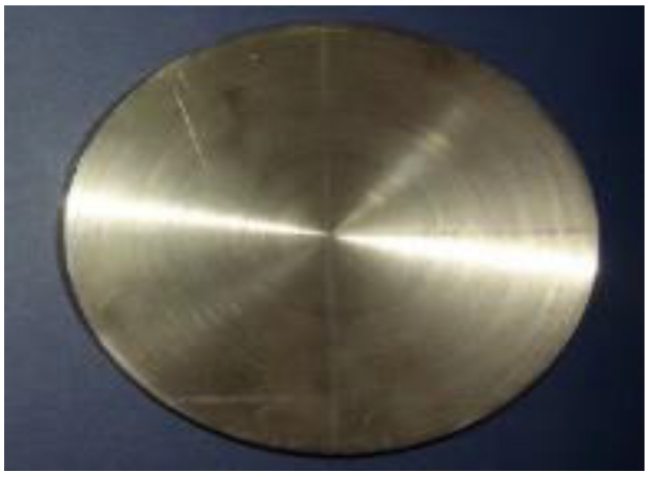

Fig. 2. Stellite 6 alloy work piece material.

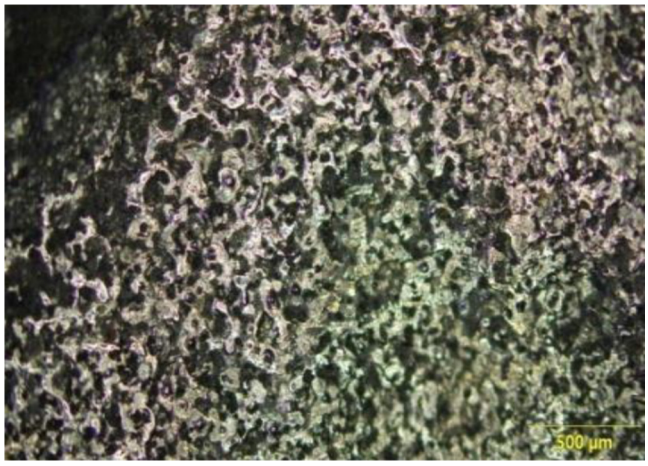

Fig. 3. Microstructure of Stellite 6 alloy work piece material.

Table 2. Control factors and levels.

Control factors	Levels	
	1	2
Aging temperature (°C)	200	400
Aging time (h.)	2	6

Table 3. Selected levels and factors (TDOE).

Levels	(A) Sliding Distance (D/m)	(B) Load (N)	(C) Sliding Speed (m/s)
1	2000	19.62	1.67
2	6000	39.24	2.51
3	10000	58.86	3.35

Table 4. Selected levels and factors (RSM).

Levels	(A) Sliding Distance (D/m)	(B) Load (L/N)	(C) Sliding Speed (m/s)
1	2000	19.62	1.67
2	10000	58.86	3.35

Fig. 4. Experimental set up.

and 20 mm diameter with 0.18 mm diameter molybdenum wire electrode material, soft water (D.M water + Gel) as dielectric fluid will be carried out using (DK7732,Concord United Pvt. Ltd., Bangalore) wire electric discharge machine" as shown in Figure 4.

Three parameters for machining Stellite 6 alloy were determined in the current study for Wire Electric discharge machining operation: Peak Current (μA), Pulse on time (μs), and Pulse off time (μs). To analyze the non-linearity influence of the process parameters, each parameter was investigated at three levels. Tables 5 and 6 show the identified control factors and their levels for TDOE and RSM.

The S/N ratio smaller the better characteristics has been used as the quality characteristic for surface roughness in this experimentation. For the elaboration of experiments plan, we used the method of L_9 Taguchi's orthogonal array (Fig. 5).

The relationship between the "output variable 'y' and the process output parameters is expressed in the form of a second degree linear polynomial regression equation" [43–45].

$$y = \beta_o + \beta_1 A + \beta_2 B + \beta_3 C + \beta_4 A^2 + \beta_5 B^2 + \beta_6 C^2 + \beta_7 AB + \beta_8 AC + \beta_9 BC + \varepsilon$$

where, β_0, β_1, β_2, ...β_9 are the regressor coefficients and ε is the random error.

Three parameters for machining Stellite 6 alloy were determined in the current study for Wire Electric discharge machining operation: Peak current (μA), Pulse on time (μs), and Pulse off time (μs). To analyze the non-linearity influence of the process parameters, each parameter was investigated at three levels. Tables 5 and 6 show the identified control factors and their levels for TDOE and RSM. These analyses are carried out for a significant level of 5%, i.e., for a level of confidence of 95% [45].

Table 5. Selected levels and factors (TDOE).

Levels	(A) Peak current (A)	(B) Pulse on time (microns)	(C) Pulse off time (microns)
1	8	100	50
2	10	200	100
3	12	300	150

Table 6. Selected levels and factors (RSM).

Levels	(A) Peak Current (A)	(B) Pulse on Time (microns)	(C) Pulse off Time (microns)
1	8	100	50
2	12	300	150

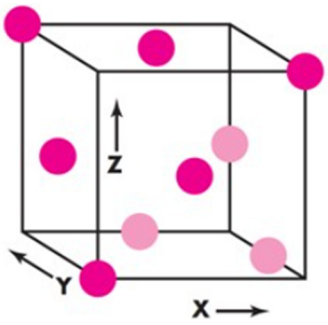

Fig. 5. L_9Orthogonal array.

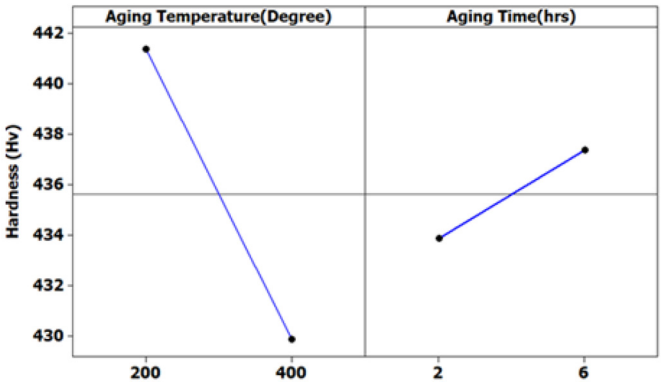

Fig. 6. Main effects plot for hardness (Hv).

Desirability function is proved to be a simultaneous optimization technique to solve multi response problems [46]. In this research objective function initially transforms the existing values in to a scale free value called desirability. Further optimum level of parameters is evaluated by composite desirability to satisfy selected process output parameters by "MINITAB 15 software".

The surface profile traces of the machined work-pieces were obtained using "Taylor/Hobson Surtronoic 3+ surface roughness measuring instrument" and age hardened workpiece, worn surface and machined workpiece surface under different condition was observed using Trinocular Inverted Metallurgical Microscope and Olympus BX53M System Microscope.

3 Results and discussions

Knowing the inadequate attention paid to the study on Stellite 6 alloy to improve its tribological behavior such as hardness (Hv), wear (mm^3) and surface roughness (microns), the experiment based on Taguchi's design of Experiments followed by Response Surface Methodology and Desirability functional approach has been discussed in the following subsections. Microstructural analysis after age hardening, worn surface and machined surface has also been discussed.

3.1 Hardness

The Stellite 6 alloy specimen is first heat treated at 950 °C for 3 h followed by water quenching at room temperature. The hardness obtained after heat treatment was 395 Hv. The specimen was then age hardened based on L_{16} orthogonal array TDOE to achieve the peak hardness value.

From the main effects plot Figure 6 for hardness indicates the optimum aging conditions for obtaining peak hardness value was, Aging Temperature (A): 200 °C and Aging Time (B): 6 h for Stellite 6 alloy.

Figure 7 shows the hardness interaction plot obtained from Taguchi's design of experiments for different aging conditions. From the interaction plot it was observed that aging temperature of 200 °C and aging time of 6 hrs gave the highest hardness value for Stellite 6 alloys. Figure 8 shows the 3D Scatter plot for Hardness (Hv) obtained from Taguchi's design of experiments under different aging conditions. Figure 9 shows the Probability plot for Hardness (Hv) obtained from Taguchi's design of experiments under different aging conditions. From the Probability plot it was observed that aging temperature of 300 °C and aging time of 4 hrs gave the highest hardness value (444.8 Hv) for Stellite 6 alloys having percentage contribution of 89%.

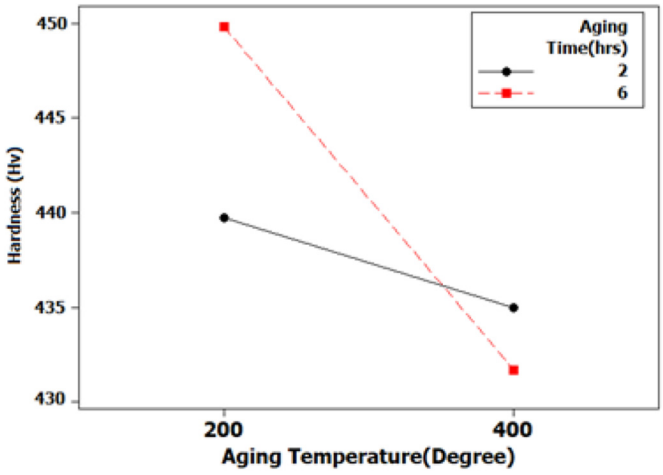

Fig. 7. Interaction plot for hardness (Hv).

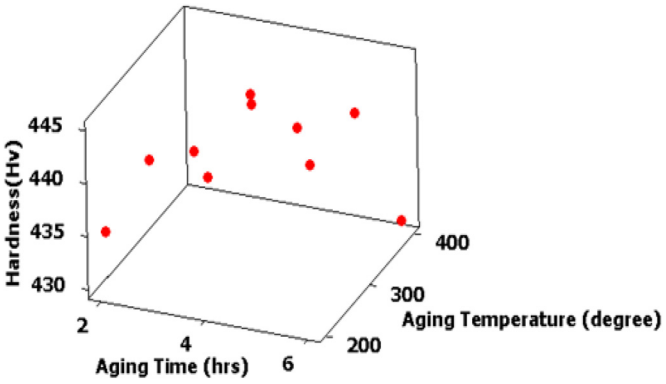

Fig. 8. 3D Scatter plot for hardness (Hv).

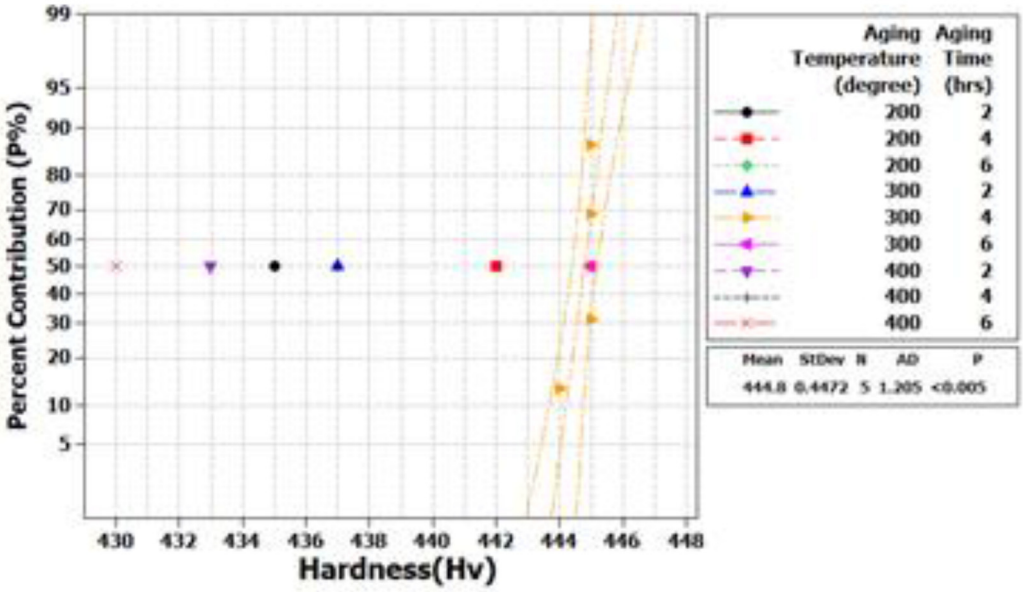

Fig. 9. Probability plot for hardness (Hv).

A second-order model has been established for hardness using response surface methodology can be used to study and analyze the hardness in any experimental domain.

$$Hardness\,(Hv) = 358.695 + 0.43A + 13.0B - 6.48 \times 10^{-04} A^2 - 0.74\,B^2 - 0.018AB$$

Figure 10 shows the hardness (Hv) variation using contour and surface plot under different aging temperature and aging time of Stellite 6 alloy. From the contour and surface plot it was observed that increase of aging time (4–6 h) and aging temperature (200–300 °C) resulted as optimum aging parameters for obtaining maximum peak hardness value. Similar observation is obtained in overlaid contour plot for Hardness(Hv) of Stellite 6 alloy under different aging temperature and aging time (Fig. 11).

From the results obtained for hardness (Fig. 12) using DFA, it is observed that optimal peak hardness value of 446.435 Hv for Stellite 6 alloy is set ataging temperature 248.48 °C and aging time 5 h.

Figures 13a–13c shows the microstructural changes occurred under different aging conditions. From Figures 13a–13c we can observe that as aging temperature and aging time increases the dendritic microstructure refinement leads to the decrease in spacing, which contributes to the high hardness values.

3.2 Wear

Wear rate behaviour of the age hardened Stellite 6 alloy having peak hardness value of 446.435 H_v obtained ataging temperature 248.48 °C and aging time 5 hrs has been used

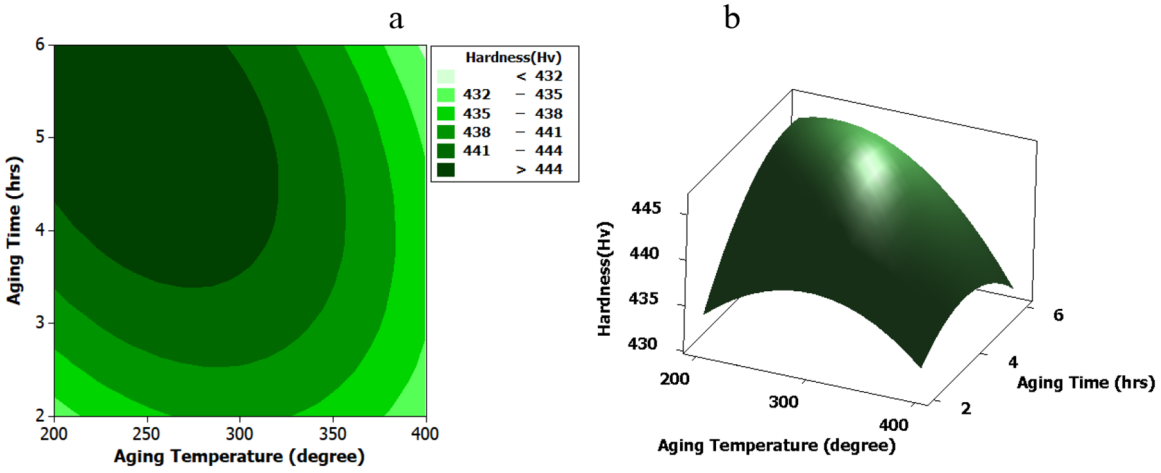

Fig. 10. Hardness contour and surface plot of Stellite 6 alloy under different aging temperature and aging time.

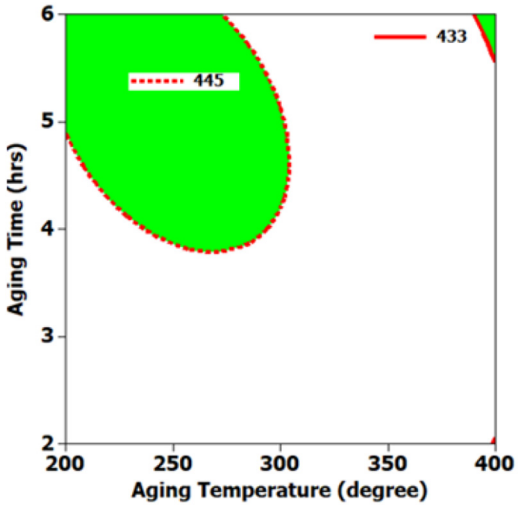

Fig. 11. Overlaid Contour plot for Hardness(Hv)of Stellite 6 alloy under different aging temperature and aging time.

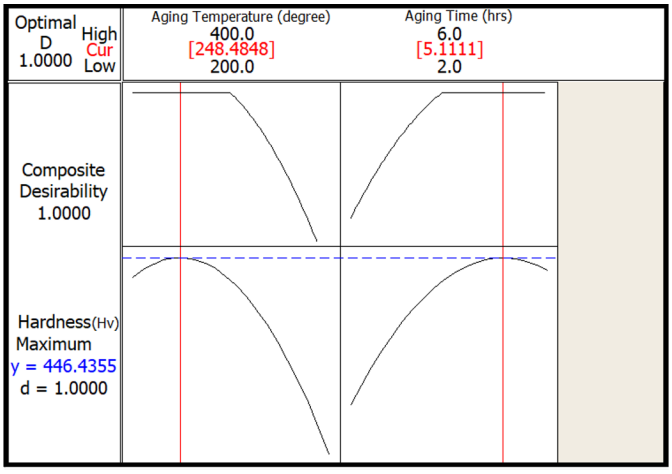

Fig. 12. Plot of composite desirability factor.

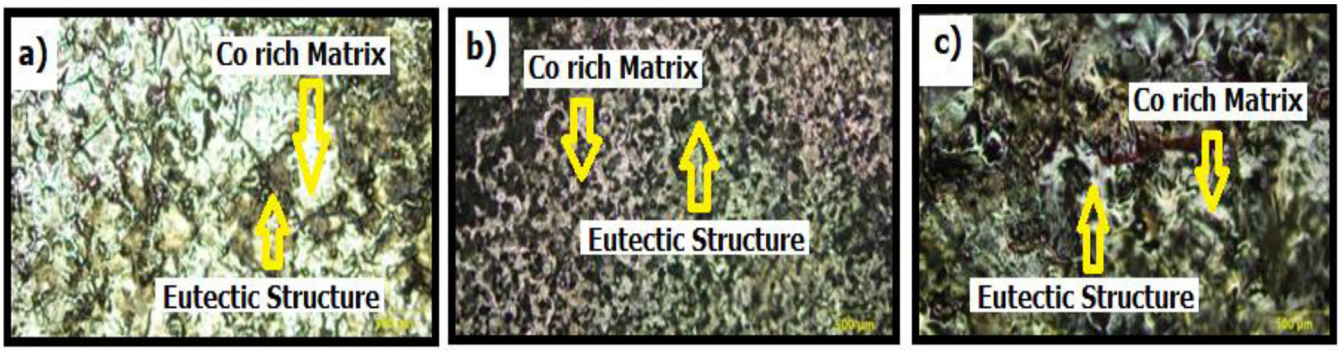

Fig. 13. Microstructural changes (a) aging temperature (200 °C) and aging time (2 h); (b) aging temperature (400 °C) and aging time (2 h) (c) aging temperature (400 °C) and aging time (6 hrs).

to study wear behaviour. The Sliding distance (D/m), Load (L/N) and Sliding Speed (m/s) has been used as process input wear parameters. The experiment is based on L_9orthogonal array to obtain optimum condition for minimising wear.

From the study, the influence of sliding distancesuch as 2000 (D/m), 6000 (D/m), 10000 (D/m) on wear of Stellite 6 alloy, it has been observed that wear rate of Stellite 6 alloy increases with increase in sliding distance. This is because at higher sliding distance, the temperature increases, which

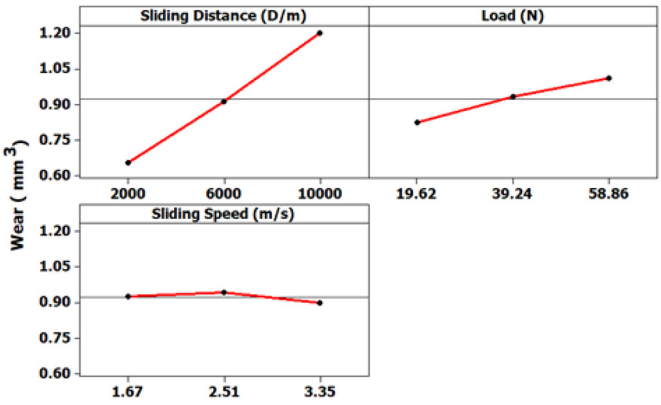

Fig. 14. Main effects plot for wear (mm^3).

Table 7. Analysis of variance for wear (mm^3).

Source	DF	Seq SS	Adj SS	Adj MS	*F*	*P*	*P*%
Sliding distance (D/m)	2	41.9682	41.9682	20.9841	39.74	0.025	89.8
Load (N)	2	4.7074	4.7074	2.3537	4.46	0.183	10.08
Sliding speed (m/s)	2	0.0413	0.0413	0.0206	0.04	0.962	0.093
Residual error	2	1.0560	1.0560	0.5280			
Total	8	47.7729					

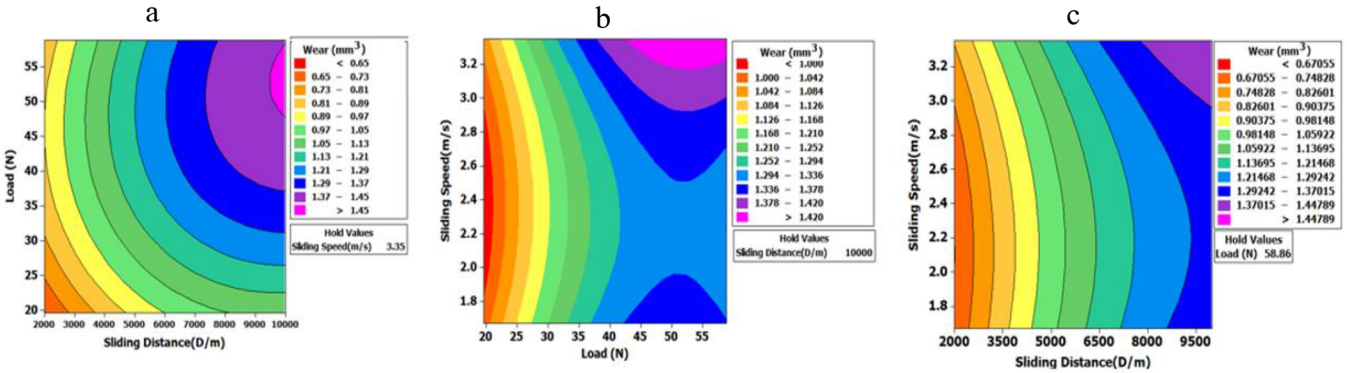

Fig. 15. Wear contourplot of Stellite 6 alloy under different conditions.

results in thermal softening, solid solution matrix, cracking and fracture of the solution matrix (carbides) further it has also been observed that the abrasive wear rate increases with increase in loaddue to temperature oxidation, frictional heat and oxide film breaks down under all testing condition. Thus it can be concluded that, minimum load, sliding distance and sliding speed is very effective in improving its wear resistance.

From the main effects plot shown in Figure 14 for wear (mm^3), indicates the optimum wear conditions for obtaining minimum wear which can be established at, Sliding distance (2000 D/m), Load (19.62 N) and Sliding Speed (3.35 m/s) for Stellite 6 alloy.

Analysis of variance for wear (Tab. 7) is an easiest technique for identifying percentage of contribution (P%) and examining wear under different wear conditions. From

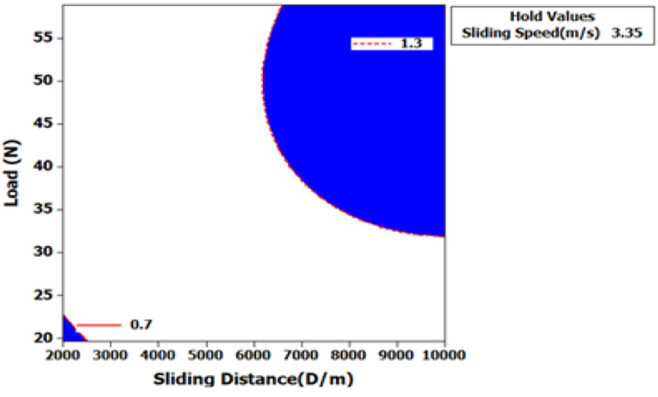

Fig. 16. Overlaid contour plot for wear (mm^3).

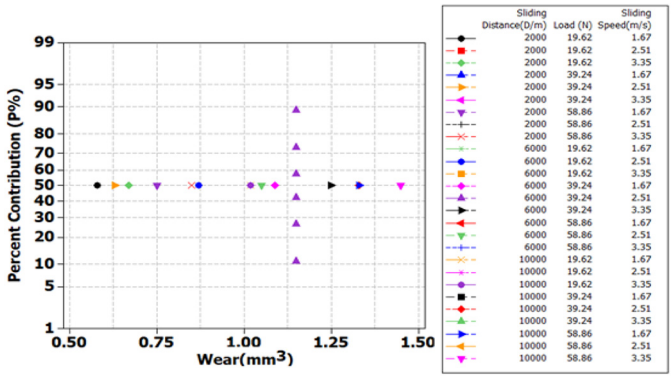

Fig. 17. Probability plot for wear (mm^3).

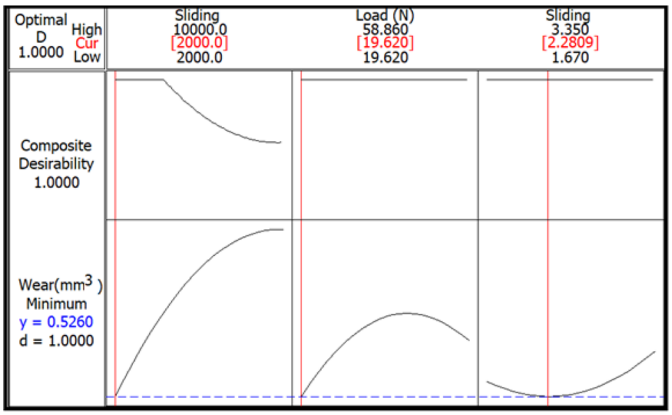

Fig. 18. Plot of composite desirability factor.

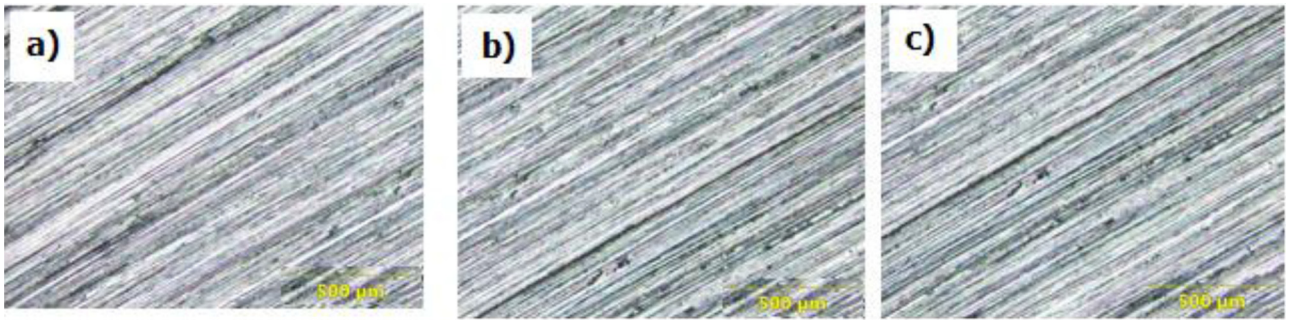

Fig. 19. Microstructural changes of worn specimen (a) sliding distance (2000 D/m), load (58.86 N) and sliding speed (3.35 m/s); (b) sliding distance (6000 D/m), load (19.62 N) and sliding speed (3.35m/s); (c) sliding distance (10,000 D/m), load (19.62 N) and sliding speed (3.35 m/s).

ANOVA it is observed that, sliding distance and load had the maximum contribution of about 89.8% and 10.08%. Hence sliding distance is considered to be an important factor, followed by load. sliding speed had a very less contribution on wear of Stellite 6 alloy".

The second-order model for wear, using response surface methodology is given below for predicting wear in any experimental domain.

$$\begin{aligned}\text{Wear}\,(\text{mm}^3) = {} & 0.394 + 0.00013A + 0.027B - 0.49C \\ & -7.24 \times 10^{-09}A^2 - 3.53 \times 10^{-04}B^2 + 0.105C^2 \\ & + 6.211 \times 10^{-07}AB - 2.604 \times 10^{-06}AC \\ & + 0.00098BC.\end{aligned}$$

Figure 15 shows the wear (mm^3) contour plot under different wear conditions of Stellite 6 alloy. From the contour plot it was observed that increase of sliding distance (2000–10000 hrs) and load (19.62–58.86 N) resulted in maximum wear value. Similar observation is obtained in overlaid contour plot for wear (mm^3) of Stellite 6 alloy under different sliding distance, load and sliding speed (Fig. 16). Figure 17 shows the probability plot for wear (mm^3) obtained from Taguchi's design of experiments for different wear conditions. From the Probability plot it was observed that sliding distance of 2000 D/m, load of 19.62N and sliding speed of 1.67 m/s gave the minimum wear value (0.58 mm^3) for Stellite 6 alloys having percentage contribution of 50%.

From the results obtained for wear (Fig. 18) using DFA it is observed that optimal wear value of 0.526 mm^3 for Stellite 6 alloy is set atsliding distance of 2000 D/m, load of 19.62N and sliding speed of 2.28 m/s. Figures 19a–19c shows the microstructural changes of worn specimen under different wear conditions.

3.3 Surface roughness

Surface roughness study has been the most important criteria for improving the mechanical properties such as fatigue life, corrosion and wear resistance. Hence in this section WEDM of the age hardened at Stellite 6 alloy having peak hardness value of 446.435 Hv has been carried out under different machining conditions such as Peak current (A), Pulse on time (microns) and Pulse off time (microns) using L_9orthogonal array.

From the main effects plot Figure 20 for surface roughness, indicates the optimum machining conditions for improving surface roughness are, peak current (12A), Pulse on time (300 microns) and pulse off time (150 microns) for

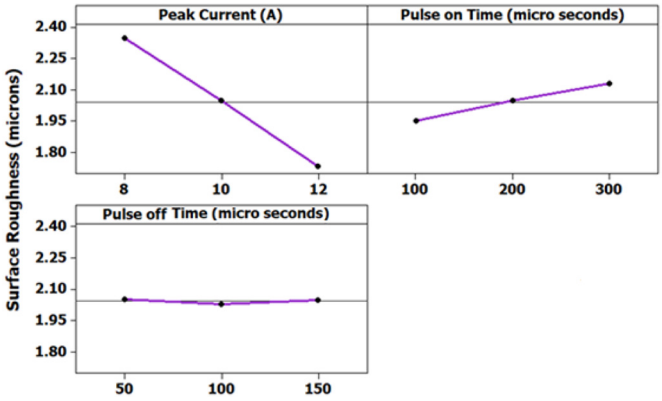

Fig. 20. Main effects plot for surface roughness (microns).

Table 8. ANOVA for surface roughness (microns).

Source	DF	Seq SS	Adj SS	Adj MS	*F*	*P*	*P*%
Peak current (A)	2	10.4184	10.4184	5.2092	1541.7	0.001	91.9
Pulse on time (microns)	2	0.8826	0.8826	0.441	130.62	0.008	7.89
Pulse off time (microns)	2	0.0238	0.0238	0.011	3.52	0.221	0.21
residual error	2	0.0068	0.0068	0.003			
Total	8	11.3315					

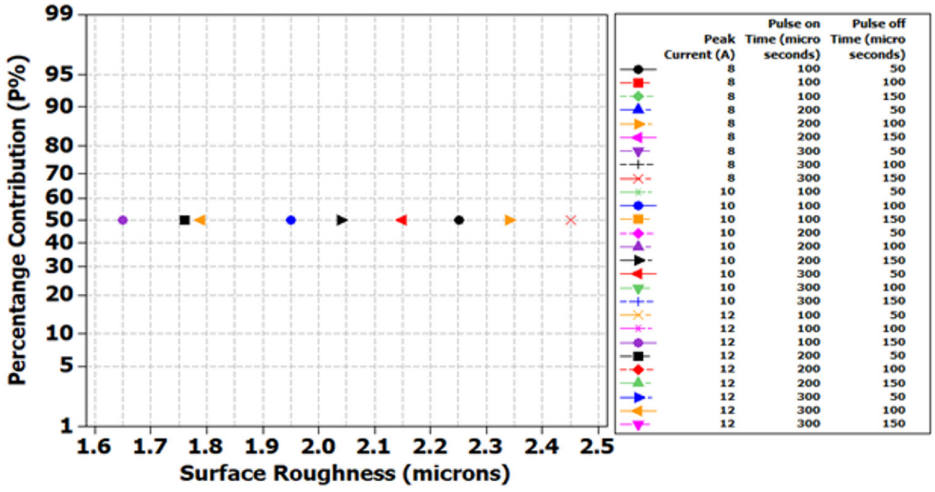

Fig. 21. Probability plot for surface roughness (microns).

Stellite 6 alloy. This is due to the fact that as the peak current (A), pulse on time (microns) and pulse off time (microns) increases plasma channel induced between the wire electrode and workpiece material results in metallurgical alterations, residual tensile stresses and easy cracking which is the results of improved surface roughness.

From ANOVA for surface roughness (microns) (Tab. 8), it is observed peak current (12A) and pulse on time (300 microns) had the maximum contribution of about 91.9% and 7.89%. Pulse off time (0.21%) had a very less contribution on surface roughness during WEDM of Stellite 6 alloy.

Figure 21 shows the Probability plot for surface roughness (microns) obtained from Taguchi's design of experiments for different machining conditions. From the Probability plot it was observed that peak current of 12 A, Pulse on Time of 100 microns and Pulse of Time of 150 microns gave the minimum surface roughness value (1.65 microns) for Stellite 6 alloys having percentage contribution of 50%.

The second-order model for wear using response surface methodology given below can be adopted for predicting surface roughness(microns) in any experimental domain.

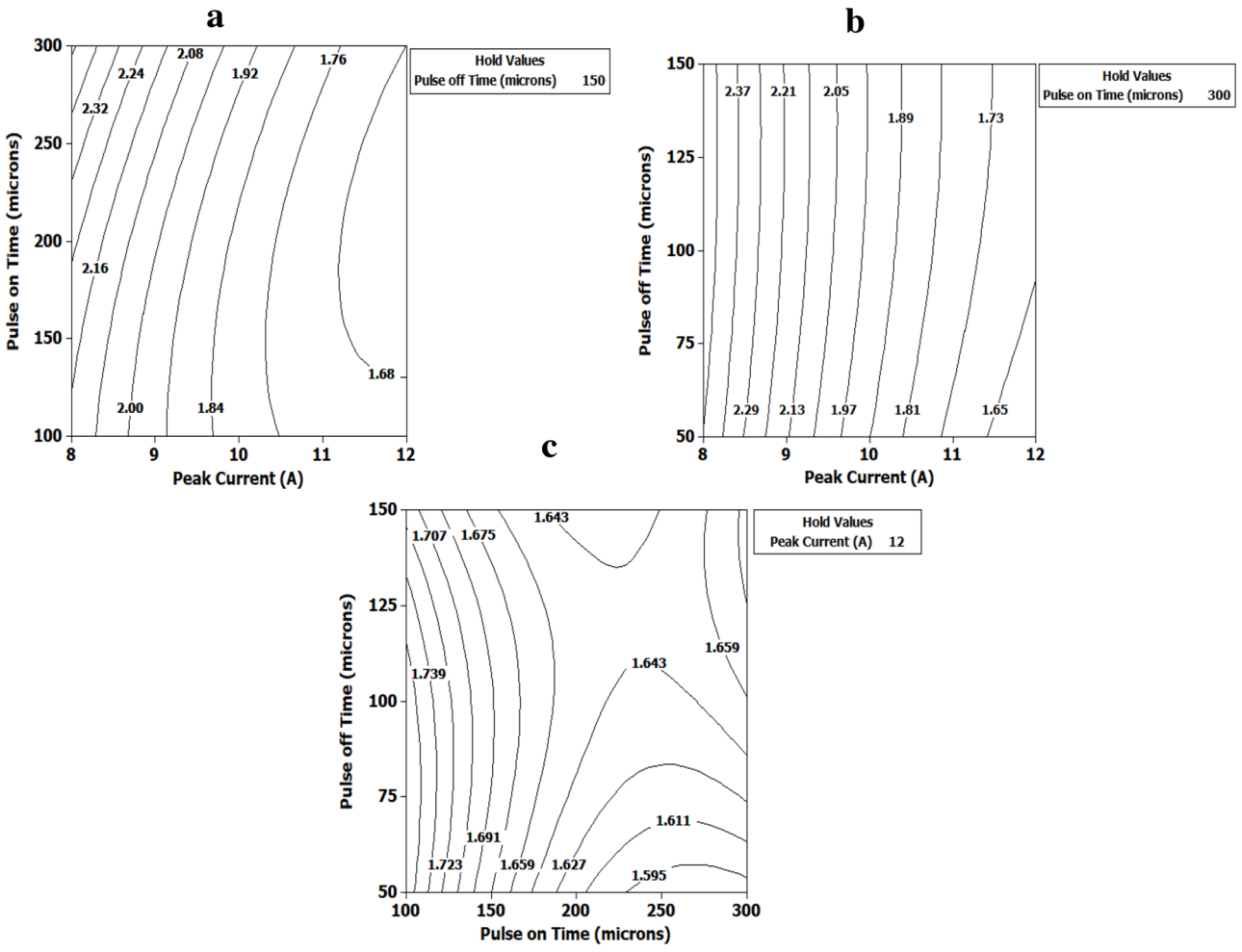

Fig. 22. Surface roughness (microns) contour lines of Stellite 6 alloy under different machining conditions.

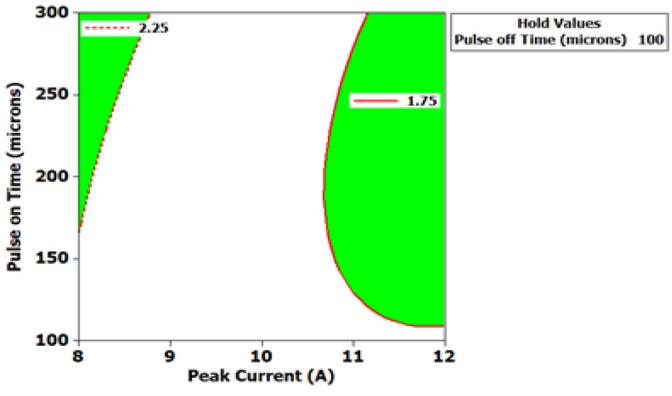

Fig. 23. Overlaid contour plot for surface roughness (microns) of Stellite 6 alloy under different machining conditions.

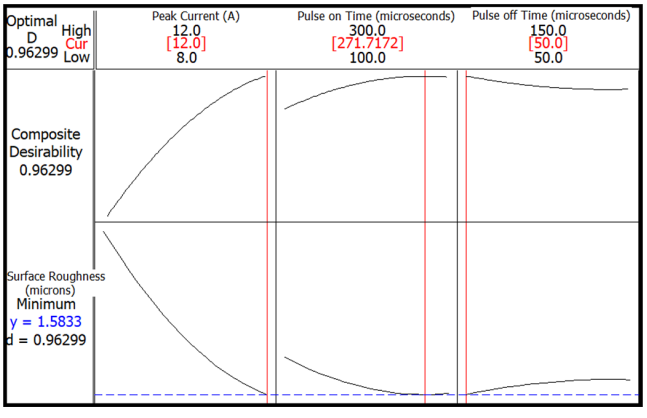

Fig. 24. Plot of composite desirability factor for surface roughness (microns).

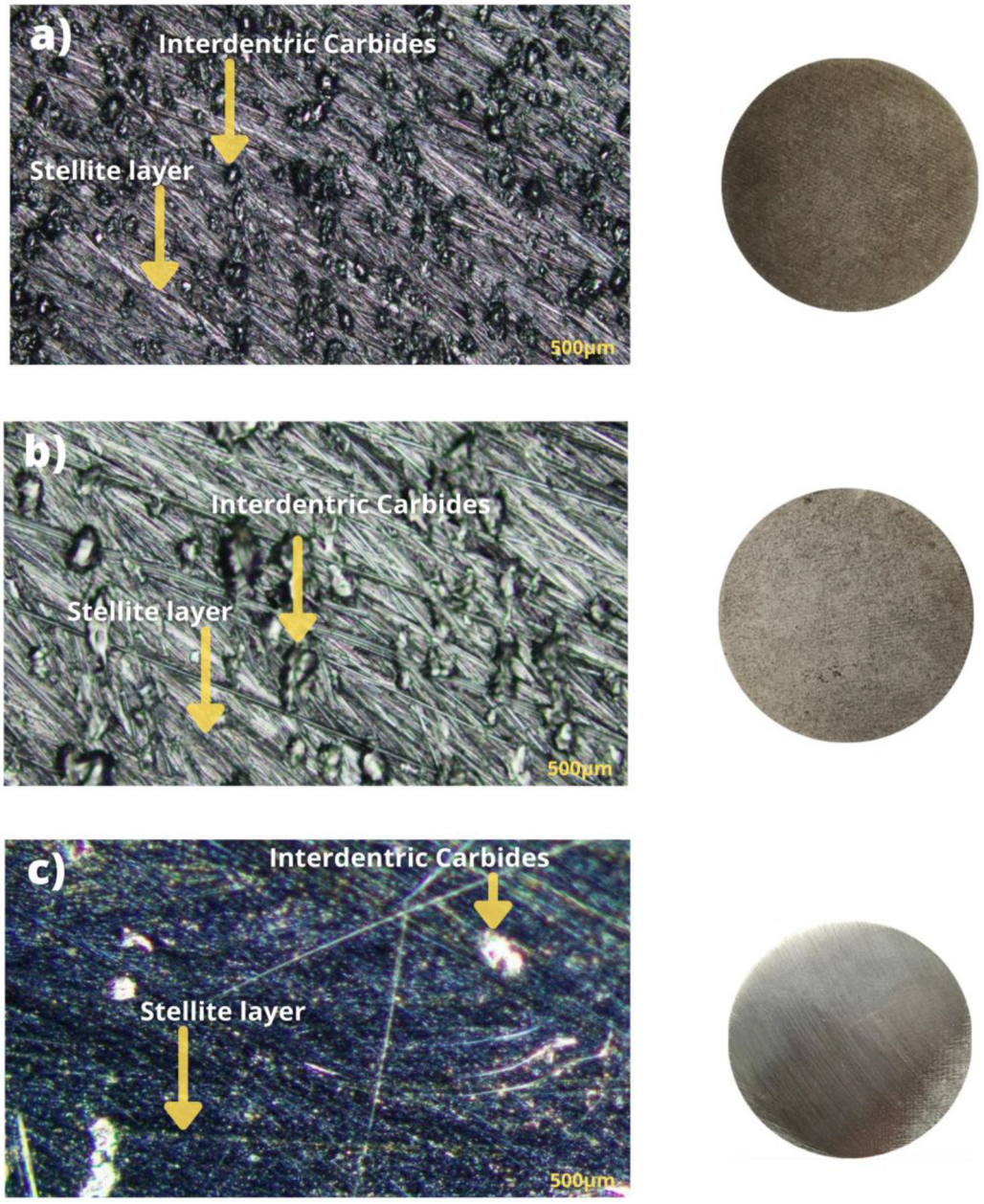

Fig. 25. Microstructural changes (a) peak current (8A), pulse on time (300 microns) and pulse off time (150 microns) (b) peak current (10A), pulse on time (300 microns) and pulse off time (150 microns) (c) peak current (12A), pulse on time (300 microns) and pulse off time (150 microns).

$$\begin{aligned}\text{Surface Roughness}\,(microns) &= 5.92064 - 0.7026A \\ &-0.022B - 4.53 \times 10^{-04}C + 0.03A^2 + 6.09 \\ &\times 10^{-06}B^2 - 9.63 \times 10^{-06}C^2 - 4.875 \times 10^{-04}AB \\ &- 0.0001AC - 7 \times 10^{-06}BC.\end{aligned}$$

Figure 22 shows the surface roughness(microns)contour lines under different machining conditions of Stellite 6 alloy. From the contour line it was observed that increase of peak current (8A to 12A) and pulse on time (100 micronsto 300 microns) resulted in minimum surface roughness value. Similar observation is obtained in overlaid contour plot for surface roughness (microns) of Stellite 6 alloy under different machining conditions (Fig. 23).

From the results obtained for surface roughness (microns) (Fig. 24) using DFA it is observed that minimum surface roughness value of 1.5833 microns for Stellite 6 alloy is set atpeak current of 12A, pulse on time of 271.7172 microns and pulse off time of 50 microns. Figures 25a–25c shows the microstructural changes of machined surface under different machining conditions of Stellite 6 alloy. From Figures 25a–25c we can observe that as the peak current increases there is larger amount of dendritic carbides and cracking of carbides due to high plastic deformation resulting in thermal softening of

Stellite 6 alloy during wire electric discharge machining resulting in better surface roughness values.

4 Concluding remarks

Based on the tribological behavior such as hardness, wear and surface roughness of Stellite 6 alloy using TDOE, RSM and DFA followed by microstructural analysis, the following conclusions can be drawn:

- From the main effects, interaction and 3D scatter plot for hardness it was observed that the optimum aging conditions for obtaining peak hardness value was, aging temperature (200 °C) and aging time (6 h) for Stellite 6 alloy. Probability plot for hardness (Hv) obtained from Taguchi's design of experiments under different aging conditions, it was observed that aging temperature of 300 °C and aging time of 4 h gave the highest hardness value (444.8 Hv) for Stellite 6 alloys having percentage contribution of 89%.
- From DFA, it is observed that optimal peak hardness value of 446.435 Hv for Stellite 6 alloy is set at aging temperature 248.48 °C and aging time 5 h.
- From microstructural changes occurred under different aging conditions, we can observe that as aging temperature and aging time increases the dendritic microstructure refinement leads to the decrease in spacing, which contributes to the high hardness values.
- From the study, the influence of sliding distance such as 2000 (D/m), 6000 (D/m), 10000 (D/m) on wear of Stellite 6 alloy, it has been observed that wear rate of Stellite 6 alloy increases with increase in sliding distance. This is because at higher sliding distance, the temperature increases, which results in thermal softening, solid solution matrix, cracking and fracture of the solution matrix (carbides) further it has also been observed that the abrasive wear rate increases with increase in load due to temperature oxidation, frictional heat and oxide film breaks down under all testing condition. Thus it can be concluded that, minimum load, sliding distance and sliding speed is very effective in improving its wear resistance. From the main effects plot it is observed that optimum wear conditions for obtaining minimum wear was Sliding distance (2000 D/m), Load (19.62 N) and Sliding Speed (3.35 m/s) for Stellite 6 alloy. From ANOVA, it is observed that, sliding distance and load had the maximum contribution of about 89.8% and 10.08%. Hence sliding distance is considered to be an important factor, followed by load. Sliding speed had a very less contribution on wear of Stellite 6 alloy.
- From the Probability plot it was observed that sliding distance of 2000 D/m, load of 19.62N and sliding speed of 1.67 m/s gave the minimum wear value (0.58 mm^3) for Stellite 6 alloys having percentage contribution of 50%.
- From the results obtained for wear using DFA it is observed that optimal wear value of 0.526 mm^3 for Stellite 6 alloy is set atsliding distance of 2000 D/m, load of 19.62 N and sliding speed of 2.28 m/s.
- From the main effects plot for surface roughness, indicates the optimum machining conditions for improving surface roughness are, peak current (12A), pulse on time (300 microns) and pulse off time (150 microns) for Stellite 6 alloy. This is due to the fact that as the peak current (A), pulse on time (microns) and pulse off time (microns) increases plasma channel induced between the wire electrode and workpiece material results in metallurgical alterations, residual tensile stresses and easy cracking which is the results of improved surface roughness.
- From ANOVA for surface roughness (microns), it is observed peak current (12A) and pulse on time (300 microns) had the maximum contribution of about 91.9% and 7.89%. Pulse off time (0.21%) had a very less contribution on surface roughness during WEDM of Stellite 6 alloy. From the Probability plot it was observed that peak current of 12 A, Pulse on Time of 100 microns and Pulse of Time of 150 microns gave the minimum surface roughness value (1.65 microns) for Stellite 6 alloys having percentage contribution of 50%.
- From the results obtained for surface roughness (microns) using DFA, it is observed that minimum surface roughness value of 1.5833 microns for Stellite 6 alloy is set at peak current of 12A, pulse on time of 271.7172 microns and pulse off time of 50 microns.
- From microstructural observation, as the peak current increases there is larger amount of dendritic carbides and cracking of carbides due to high plastic deformation resulting in thermal softening of Stellite 6 alloy during wire electric discharge machining resulting in better surface roughness values.
- The second-order model for hardness, wear and surface roughness using response surface methodology can be adopted for predicting for hardness, wear and surface roughness in any experimental domain.

References

1. C. Sponaugle, Pittsburgh Engineer, Quarterly publication of the Engineers' Society of Western Pennsylvania Winter (2005) pp. 7–9.
2. M.S. Hasan, M.A. Mazid, R.E. Clegg, The basics of stellites in machining perspective, Int. J. Eng. Mater. Manufact. **1** (2016) 35–50
3. W. Betteridge, Cobalt and Its Alloys (Halted Press, Chichester, 1982)
4. L. Fouilland, M. El Mansori, M. Gerland, Role of welding process energy on the microstructural variation in a cobalt-based superalloy hardfacing, Surface Coat. Technol. **201** (2007) 6445–6451
5. Z. Barsoum, A. Lundback, Simplified FE welding simulation of fillet welds – 3D effects on the formation of residual stresses, Eng. Fail. Anal. **16** (2009) 2281–2289
6. Z. Xueping, G. Erwei, C.R. Liu, Optimisation of process parameter of residual stresses for hard turned surfaces, J. Mater. Process. Technol. **209** (2009) 4286–4291

7. R. Kaul, P. Ganesh, M.K. Tiwari, A.K. Singh, P. Tripathi, A. Gupta, A.K. Nath, Laser assisted deposition of graded overlay of Stellite 6 on austenitic stainless steel, Laser Eng. **12** (2002) 207–225
8. C.T. Sims, Cobalt-Base Alloys, the Superalloys (John Wiley and Sons), 145
9. M.X. Yao, J.B.C. Wu, W. Xu, R. Liu, Metallographic study and wear resistance of a high-C wrought Co-based alloy Stellite 706K, Mater. Sci. Eng. A **407** (2005) 291–298
10. Z. Ruml, F.A. Straka, New model for steam turbine blade materials erosion, Wear **186-187** (1995) 421–424; 14. C. Zhao, F. Tian, H.R. Peng, & Hou, J.Y. (2002). Non-transferred arc plasma cladding of stellite Ni60 alloy on steel. Surface and Coatings Technology, **155**(1), 80-84.
11. M.S. Hasan, A.M. Mazid, R.E. Clegg, Optimisation of the machining of stellite 6 PTA hardfacing using surface roughness, Key Eng. Mater. **443** (2010) 227–231
12. M.S. Hasan, A.M. Mazid, R.E. Clegg, Effect of cutting tool nose radius on surface roughness for Stellite 6 machining using coated carbide insert, in Proc. of the 6th Australian Congress on Applied Mechanics (ACAM 6 2010), Perth, Australia (2010) 603–612
13. M.S. Hasan, A.M. Mazid, R.E. Clegg, A. McLeod, Residual stress analysis on machined surface in turning Stellite 6, in Proc. of the 6th Australian Congress on Applied Mechanics (ACAM 6 2010), Perth, Australia (2010) pp. 714–722
14. M.S. Hasan, Optimisation of machining processes design for stellite 6, a wear resistant and difficult-tomachine material. Master of Engineering thesis, Central Queensland University, Rockhampton, Australia (2011) p. 136
15. C.P. Sullivan, M.J. Donachie, Jr, Cobalt -Base Superalloys, Cobalt Information Center, Brussels, Belgium (1979)
16. L. Zixiang, C. Yinan, W. Jie, L. Changmeng, W. Jiachen, X. Tianqiu, Characterization of microstructure and mechanical properties of Stellite 6 part fabricated by wire arc additive manufacturing, MDPI-metals3 **223–227** (2019) 2019
17. A. Marti, Cobalt-base alloys used in bone surgery. Injury **31** (2000) 18–21
18. Y.S. Wong, M. Rahman, H.S. Lim, H. Han, N. Ravi, Investigation of micro-EDM material removal characteristics using single RC-pulse discharges, J. Mater. Process. Technol. **140** (2003) 303–307
19. A.S. D'Oliveira, C.M. Da Silva, Microstructural features of consecutive layers of stellite 6 deposited by laser cladding, Surf. Coat. Technol. **153** (2002) 203–209
20. R.S. Pawade, S.S. Joshi, P.K. Brahmankar, Effect of machining parameters and cutting edge geometry on surface integrity of high-speed turned Inconel 718, Int. J. Mach. Tools Manufact. **48** (2008) 15–28
21. J.C. Outeiro, J.C. Pina, R. M'Saoubi, F. Pusavec, I.S. Jawahir, Analysis of residual stresses induced by dry turning of difficult-to-machine materials, CIRP Ann. Manufactur. Technol. **57** (2008) 77–80
22. M. Salio, T. Berruti, G. De Poli, Prediction of residual stress distribution after turning in turbine disks, Int. J. Mech. Sci. **48** (2006) 976–984
23. L. Wang, D. Li, Effects of yttrium on microstructure, mechanical properties and high temperature wear behaviour of cast Stellite 6 alloy, Wear **255** (2003) 535–544
24. H. Celik, M. Kaplan, Effects of silicon on the wear behaviour of cobalt-based alloys at elevated temperature, Wear **257** (2004) 606–611
25. K. Egashira, A. Matsugasako, H. Tsuchiya and M. Miyazaki, Electrical discharge machining with ultralow discharge energy, J. Precis. Eng. **30** (2006) 414–420
26. Y.B. Jia, J.N. Kim, Experimental investigations into near-dry milling EDM of Stellite alloys, Materials Science, Int. J. Mach. Mach. Mater. **7** (2010) 96–111
27. S. Raviraj, B.V. Augustine, K. Laxmikanth, Empirical study on stress distribution zone during machining of DRACs using finite element analysis, Taguchi's design of experiments and response surface methodology, ARPN J. Eng. Appl. Sci. **14** (2019) 2576–2582
28. S. Raviraj, P. Raghuvir, R. Srikanth, K. Vasanth, Study on surface roughness minimization in turning of DRACs using surface roughness methodology and Taguchi under pressured steam jet approach, ARPN J. Eng. Appl. Sci. **3** (2008) 59–67
29. S. Raviraj, P. Raghuvir, S.R. Srikanth, Tribological studies on discontinuously reinforced aluminium composites based on the orthogonal arrays, ARPN J. Eng. Appl. Sci. **3** (2008) 94–92
30. P.K. Shetty, R. Shetty, D. Shetty, N.F. Rehaman, Machinability study on dry drilling of titanium alloy Ti-6Al-4V using L9 orthogonal array, Proc. Mater. Sci. **5** (2014) 2605–2614
31. S. Raviraj, K.J. Tony, D.R. Goutam, S.R. Srikanth, Surface roughness analysis during turning of Ti-6Al-4V under near dry machining using statistical tool, Int. J. Curr. Eng. Technol. **4** (2014) 2061–2067
32. D.C. Montgomery, Design and Analysis of Experiments, sixth edition, John Wiley & sons, Inc. (2005)

Cite this article as: Karthik S.R., Neelakanta V. Londe, Raviraj Shetty, Rajesh Nayak, Adithya Hedge, Optimization and prediction of hardness, wear and surface roughness on age hardened stellite 6 alloys, Manufacturing Rev. **9**, 10 (2022)